

Molten carbonate fuel cells: contribution to the study of cathode behaviour and oxygen reduction in molten $\text{Li}_2\text{CO}_3\text{--K}_2\text{CO}_3$ at 650 °C

M. Cassir¹, B. Malinowska, C. Canevet, L. Sportouch, J. Devynck

*Ecole Nationale Supérieure de Chimie de Paris, Laboratoire d'Electrochimie et de Chimie Analytique LECA (Unité Associée au CNRS URA 216),
11 rue Pierre et Marie Curie, 75231 Paris, Cedex 05, France*

Abstract

A contribution to the understanding of the complex behaviour of the cathode in molten carbonate fuel cells, focussing on the oxygen reduction mechanism and the lithiation process, is presented in this paper. As a first step, the thermodynamic stability ranges of oxygen and nickel species are established. The electrochemical behaviour of superoxide and oxide species, unstable in the carbonate melt but locally created in the diffusion layer, is investigated according to the acidity conditions. Nickel recovered in situ by nickel oxide is analysed by X-ray diffraction and voltammetric techniques. The lithiation and dissolution of nickel oxide are more particularly described.

Keywords: Molten carbonate fuel cells; Oxygen systems; Nickel oxide; Reduction; Lithiation; Dissolution

1. Introduction

The improvement of the lifetime of molten carbonate fuel cells (MCFCs) requires a better understanding of two important aspects occurring at the cathode: (i) the oxygen reduction mechanism, and (ii) the corrosion of the state-of-the-art nickel cathode recovered by nickel oxide.

Although it is well known that the reduction process involves reduced oxygen species, such as O_2^- , O_2^{2-} (or O^-), there are several controversial interpretations in the literature, see Refs. [1,2]. On the one hand, we have postulated that this complexity could be due to the fact that, under the acidic MCFC conditions (high $p\text{CO}_2$), these species do not exist quantitatively in the bulk of the molten eutectic because of their thermodynamic instability. On the other hand, we have characterized in most of the carbonate eutectics the redox systems relative to these species in basic conditions under very low $p\text{CO}_2$.

The electrochemical behaviour of the NiO/Ni cathode has been investigated by different authors, mostly in $\text{Li}_2\text{CO}_3\text{--K}_2\text{CO}_3$ melts [3–7], in $\text{Li}_2\text{CO}_3\text{--Na}_2\text{CO}_3$ [8,9], and in $\text{Li}_2\text{CO}_3\text{--Na}_2\text{CO}_3\text{--K}_2\text{CO}_3$ in the authors' laboratory [10]. Nevertheless, the determination by electrochemical techniques of the NiO solubility and a precise description of the lithiation phenomenon have not yet been achieved in $\text{Li}_2\text{CO}_3\text{--K}_2\text{CO}_3$ eutectic.

Our principal aim in this work was to establish, in the acidic MCFC conditions, a general frame for the study of the two mentioned aspects affecting the cathode behaviour in $\text{Li}_2\text{CO}_3\text{--K}_2\text{CO}_3$ eutectic. Different methods have been used: (i) thermodynamic predictions of the stability domains of oxygen and nickel species; (ii) voltammetric studies of the redox systems relative to oxygen reduction and lithiated nickel species, and (iii) X-ray diffraction analysis in order to give experimental evidence for the formation of lithiated nickel oxide.

2. Thermodynamic predictions

Thermochemical data for oxygen and nickel species were extracted from the literature [11–14]. Stability domains of oxygen and nickel species were established as a function of the acidity of $\text{Li}_2\text{CO}_3\text{--K}_2\text{CO}_3$ eutectic, as described in previous papers [1,10]. As no data were found concerning lithium–nickel and potassium–nickel compounds, they were not considered in the potential–acidity diagrams.

Fig. 1 shows a potential–acidity diagram of the binary eutectic at 650 °C. The limits reported are: oxidation (O_2 , O_2^{2-} or O_2^- formation), basicity (Li_2O saturation) and acidity ($p\text{CO}_2$ at 1 atm). The reduction limit was omitted. Under standard conditions, molecular oxygen ($p\text{O}_2 = 1$ atm) is stabilized under high $p\text{CO}_2$ (acidic media) and O_2^{2-} (activity: 1) under very low $p\text{CO}_2$ (basic media). At $p\text{CO}_2$ 0.1 atm, in

¹ Fax: (33) 1-44 27 67 50. e-mail: cassir@ext.jussieu.fr.

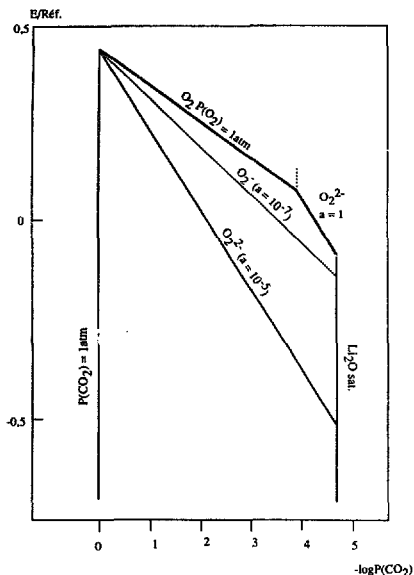


Fig. 1. Electrochemical stability domain of oxygen species in molten $\text{Li}_2\text{CO}_3\text{-K}_2\text{CO}_3$ (42.7–57.3 mol%) at 650 °C calculated from thermochemical data [11,12].

the usual conditions of MCFCs, neither peroxide nor superoxide species can be stabilized even for activities as low as 10^{-4} . Nevertheless, these species could be present at very low activity values: 10^{-5} for peroxide and 10^{-7} for superoxide.

Fig. 2 represents the stability domains of nickel species, excluding the lithiated compounds. Although NiO is stable whatever the acidity level, a small dissolution can be observed in acidic media (NiCO_3 at an activity of about 10^{-6}).

3. Experimental

Lithium–potassium molten carbonates (42.7–57.3 m/o, or 62–38 m/o), lithium oxide and potassium superoxide were prepared from Merck reagents of analytical purity ($>98\%$). Nickel carbonate was a Strem Chemicals Inc. reagent. Electrochemical measurements were performed with an ElectroKemat potentiostatic system (E.K. E390 Model) controlled by an IBM/PS2. X-ray diffraction was carried out with a CGR type Théta 60 diffractometer using a $\text{Cu K}\alpha$ radiation ($\lambda = 1.789 \text{ \AA}$). The working microelectrodes were gold planar discs with a diameter between 1 and 1.6 mm or a nickel wire with a diameter 1 mm. Gold ultramicroelectrodes with a diameter 200 μm were described in Ref. [15]. The refer-

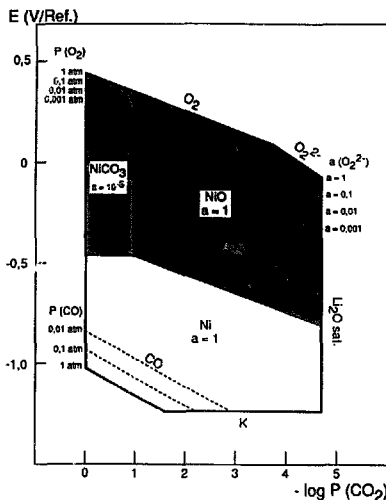


Fig. 2. Electrochemical stability domain of nickel species in molten $\text{Li}_2\text{CO}_3\text{-K}_2\text{CO}_3$ (62–38 mol%) at 650 °C calculated from thermochemical data [11–14].

ence electrode was a silver wire dipped into an Ag_2SO_4 ($10^{-1} \text{ mol kg}^{-1}$) eutectic melt. Electrochemical cell and experimental procedures were fully described in Refs. [1,10].

4. Electrochemical characterization of oxygen systems

In Fig. 3, voltammograms are reported in $\text{Li}_2\text{CO}_3\text{-K}_2\text{CO}_3$ (62–38), under $p\text{CO}_2 = 1 \text{ atm}$ for different start potentials. The reduction current at about -0.1 to 0.1 V versus Ag^+/Ag is related to the anodic limit due to the carbonate oxidation. When the start potential is lower than 0 V , no reduction current was observed. On the contrary, the current increases

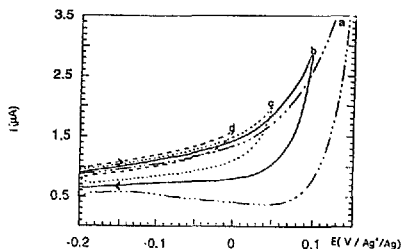


Fig. 3. Cyclic voltammograms at a gold ultramicroelectrode (surface area (S) = $1.26 \times 10^{-3} \text{ cm}^2$) in molten $\text{Li}_2\text{CO}_3\text{-K}_2\text{CO}_3$ (62–38 mol%) at 650 °C and $p\text{CO}_2 = 1 \text{ atm}$ for different start potentials: (a) 0.15 V; (b) 0.10 V; (c) 0.05 V, and (d) 0.00 V vs. Ag^+/Ag ; $\nu = 0.1 \text{ V s}^{-1}$.

Table 1

Standard potentials E^* (V) of oxygen systems at 650 °C calculated from thermochemical data [11,12]. Reference $\text{Li}_2\text{O}/\text{O}_2$

$\text{O}_2/\text{Li}_2\text{O}$	$\text{Li}_2\text{O}_2/\text{Li}_2\text{O}$	$\text{Li}_2\text{O}_2/\text{Li}_2\text{O}$	$\text{LiO}_2/\text{Li}_2\text{O}_2$	$\text{Li}_2\text{CO}_3/\text{Li}_2\text{O}_2$	$\text{Li}_2\text{CO}_3/\text{Li}_2\text{O}_2$	$\text{Li}_2\text{CO}_3/\text{O}_2$
0.00	0.280	-0.080	1.000	0.694	0.660	0.424

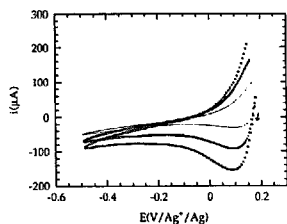


Fig. 4. Development of cyclic voltammograms at a gold electrode ($S = 2.01 \times 10^{-2} \text{ cm}^2$) in molten $\text{Li}_2\text{CO}_3\text{-K}_2\text{CO}_3$ (42.7–57.3 mol%) at 650 °C and $p\text{CO}_2 = 0.1 \text{ atm} + p\text{O}_2 = 0.9 \text{ atm}$ for scan rates, v , of 0.2, 0.8 and 1.6 V s^{-1} ; start potential = 0.18 V vs. Ag^+/Ag .

with increasing values of the start potential. This tends to prove that the reduced species proceeds from solvent oxidation and do not exist significantly in the bulk of the molten eutectic. It has been suggested in the literature [1] that the species responsible for this reduction current is either a superoxide or a peroxide species, probably created in the diffusion layer by the reaction between molecular oxygen, produced at the anodic limit, and carbonate ions. The same behaviour was observed under $p\text{CO}_2 = 0.1 \text{ atm} + p\text{O}_2 = 0.9 \text{ atm}$ and in $\text{Li}_2\text{CO}_3\text{-K}_2\text{CO}_3$ (42.7–57.3).

The development of cyclic voltammograms in the last mentioned eutectic for different scan rates is reported in Fig. 4. The plot of the reduction current with \sqrt{v} is linear, indicating that it is diffusion controlled. According to the calculated thermodynamic standard potentials given in Table 1 and to the fact that addition of potassium superoxide in the melt increased this current, it should be attributed to superoxide species.

The value of the half reduction peak width for a non-unit order system ($\text{Ox} + ne \rightleftharpoons 2\text{Red}$) [1] is in agreement with the hypothesis of a three-electron reversible process. Therefore, the reduction can be described as:



followed by the slow neutralization of oxide ions: $\text{O}^{2-} + \text{CO}_2 \rightleftharpoons \text{CO}_3^{2-}$ (the rate constant of this reaction is low enough to consider that CO_2 does not participate in the reduction mechanism [1]).

Fig. 5 represents the development of cyclic voltammograms in $\text{Li}_2\text{CO}_3\text{-K}_2\text{CO}_3$ (42.7–57.3) after addition of $5 \times 10^{-5} \text{ mol}$ of Na_2O_2 . An electrochemical system appears with a reduction peak current at -0.39 V versus Ag^+/Ag and an oxidation peak current at -0.26 V versus Ag^+/Ag . The reduction current was attributed to the peroxide species, which is in accordance with results in basic media, see Ref.

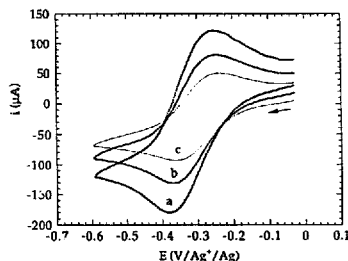


Fig. 5. Development of cyclic voltammograms at a gold electrode ($S = 2.01 \times 10^{-2} \text{ cm}^2$) in molten $\text{Li}_2\text{CO}_3\text{-K}_2\text{CO}_3$ (42.7–57.3 mol%) at 650 °C and $p\text{CO}_2 = 0.1 \text{ atm} + p\text{O}_2 = 0.9 \text{ atm}$ after addition of $5 \times 10^{-5} \text{ mol}$ Na_2O_2 : (a) 4 min; (b) 6 min, and (c) 8 min; start potential = 0 V vs. Ag^+/Ag .

[1]. This current decreased with the slow neutralization ($5 \times 10^{-6} \text{ mol s}^{-1}$) of peroxide species with CO_2 . Analysis of the redox system is in agreement with a reversible second-order non-unit reaction:



followed by the slow neutralization of oxide ions.

5. Electrochemical characterization of nickel species

Fig. 6 represents the open-circuit potential (OCP) of a nickel foil dipped in $\text{Li}_2\text{CO}_3\text{-K}_2\text{CO}_3$ (62–38) at 650 °C under $p\text{CO}_2 = 0.1 \text{ atm} + p\text{O}_2 = 0.9 \text{ atm}$. The potential was initially about -0.90 V , which may correspond to the NiO/Ni system. Then the nickel surface was recovered with NiO and the potential increased, probably because of the influence of a lithiation process [3,10]. The potential reached a stable value

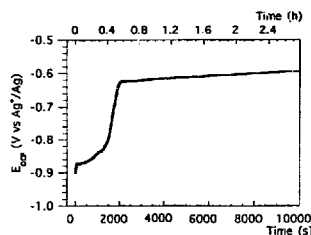


Fig. 6. Open-circuit potential of a nickel electrode in molten $\text{Li}_2\text{CO}_3\text{-K}_2\text{CO}_3$ (62–38 mol%) at 650 °C and $p\text{CO}_2 = 0.1 \text{ atm} + p\text{O}_2 = 0.9 \text{ atm}$.

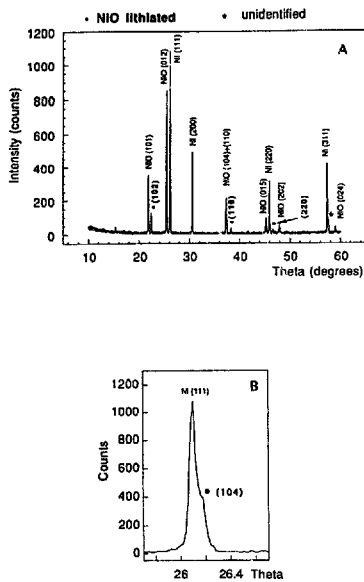


Fig. 7. X-ray diffraction pattern of a nickel foil after treatment in molten $\text{Li}_2\text{CO}_3\text{-K}_2\text{CO}_3$ (62–38 mol%) at 650°C under $p\text{CO}_2 = 0.1$ atm + $p\text{O}_2 = 0.9$ atm: (A) general diffraction pattern, and (B) detail.

after 32 min which means, according to Nishina et al. [3], that the lithium insertion in the NiO lattice should be totally achieved. After this OCP treatment, the nickel foil was removed from the molten carbonate, air-cooled, rinsed [16] and characterized by X-ray diffraction. Ni and NiO lines are reported in Fig. 7(a). Three other lines (102), (110) and (220), identified in the X-ray pattern, correspond to the lithiated compound: $\text{Li}_x\text{Ni}_{1-x}\text{O}$ [17,18]. Line (104), relative to the lithiated compound, is partially masked by line Ni(111), as shown in Fig. 7(b).

The electrochemical behaviour of a nickel electrode in the same eutectic, under the same conditions, is shown in Fig. 8. A complex reduction current is observed with the principal component at -1.22 V. The associated oxidation current, also complex, is located at about -1.02 V. The principal reduction and oxidation peak currents were plotted as a function of the scan rate. These plots are linear versus ν when $\nu < 1$ V s^{-1} (homogeneous diffusion) and linear versus $\sqrt{\nu}$ when $\nu > 2$ V s^{-1} (semi-infinite diffusion). This behaviour is characteristic for an intercalation process, according to Armand et al. [19]. The electrochemical system involved could be probably described as:

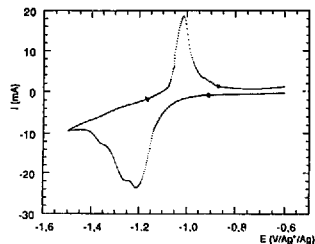
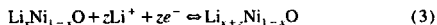


Fig. 8. Cyclic voltammogram at a nickel electrode in molten $\text{Li}_2\text{CO}_3\text{-K}_2\text{CO}_3$ (62–38 mol%) at 650°C and $p\text{CO}_2 = 0.1$ atm + $p\text{O}_2 = 0.9$ atm; $\nu = 0.05$ V s^{-1} ; start potential = -0.6 V vs. Ag^+/Ag .

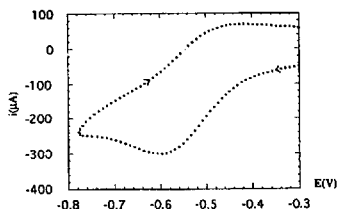


Fig. 9. Cyclic voltammogram at a gold electrode ($S: 2.01 \times 10^{-2}$ cm^2) in molten $\text{Li}_2\text{CO}_3\text{-K}_2\text{CO}_3$ (42.7–57.3 mol%) at 650°C under $p\text{CO}_2 = 1$ atm after dipping a nickel foil for 24 h; $\nu = 0.8$ V s^{-1} ; start potential = -0.3 V vs. Ag^+/Ag .

with an electrochemical intercalation–deintercalation process. Further voltammetric, impedance spectroscopy and structural studies are necessary to confirm this hypothesis.

Another system, at higher potentials, was observed with a gold electrode, as shown in Fig. 9, when a nickel foil was previously dipped during 24 h under $p\text{CO}_2 = 1$ atm in $\text{Li}_2\text{CO}_3\text{-K}_2\text{CO}_3$ (42.7–57.3). The reduction peak current occurred at -0.59 V and the oxidation peak current at -0.46 V. The same reduction^o current appeared at a gold electrode when a Ni(II) salt was added. The plot of the reduction current versus $\sqrt{\nu}$ is linear indicating that the reduction process is diffusion controlled. The peak potentials are constant whatever the scan rate, showing that the redox system involved is reversible. The value of the half reduction peak width ($E_p - E_{p/2} = 0.175/n$ at 650°C [20]) is in accordance with a two-electron reversible process. As we have demonstrated in $\text{Li}_2\text{CO}_3\text{-Na}_2\text{CO}_3\text{-K}_2\text{CO}_3$ eutectic [10], this system is relative to Ni^{2+}/Ni . The NiO solubility was determined at saturation of the melt from the slope of lp versus $\sqrt{\nu}$. The value obtained is 1.02×10^{-3} mol kg^{-1} . This result is very close to that obtained in the same melt by atomic absorption: 1.13×10^{-3} mol kg^{-1} [21].

6. Conclusions

A first approach has been made to understanding the complex behaviour of the oxygen reduction mechanism and nickel species in $\text{Li}_2\text{CO}_3\text{-K}_2\text{CO}_3$ at 650°C .

In the acidic conditions used in MCFs, we have shown that the reduced oxygen species are thermodynamically unstable but they may be present in the diffusion layer. A three-electron reversible reduction of superoxide into oxide species, followed by a slow neutralization with CO_2 , has been proposed as the most plausible mechanism.

Lithiation of nickel oxide has been characterized by spectroscopic and electrochemical techniques under $p(\text{CO}_2) = 0.1 \text{ atm} + p(\text{O}_2) = 0.9 \text{ atm}$. A hypothesis has been formulated based on the electrochemical reduction of the $\text{Li}_x\text{Ni}_{1-x}\text{O}$. The solubility of NiO has been determined under $p\text{CO}_2 = 1 \text{ atm}$.

References

- [1] M. Cassir, G. Moutiers and J. Devynck, *J. Electrochem. Soc.*, **140** (1993) 3114.
- [2] G. Moutiers, M. Cassir, C. Piolet and J. Devynck, *Electrochim. Acta*, **36** (1991) 1063.
- [3] T. Nishina, K. Takizawa and I. Uchida, *J. Electroanal. Chem.*, **263** (1989) 87.
- [4] Gang Xie, Y. Sakamura, K. Ema and Y. Ito, *J. Power Sources*, **32** (1990) 125.
- [5] Gang Xie, Y. Sakamura, K. Ema and Y. Ito, *J. Power Sources*, **32** (1990) 135.
- [6] T.D. Kaun, *Proc. 4th Int. Symp. Molten Salts, 172th Meet. Int. Soc., Hawaii, HI, USA*, 1987, p. 489.
- [7] P. Tomczyk, H. Sato, K. Yamada, T. Nishina and I. Uchida, *J. Electroanal. Chem.*, **391** (1995) 125.
- [8] P. Tomczyk, G. Mordarski and J. Oblakowski, *J. Electroanal. Chem.*, **353** (1993) 177.
- [9] L.K. Bieniasz and P. Tomczyk, *J. Electroanal. Chem.*, **353** (1993) 195.
- [10] B. Malinowska, M. Cassir, F. Delcorso and J. Devynck, *J. Electroanal. Chem.*, **389** (1995) 21.
- [11] *JANAF Thermochemical Tables*, US Department of Commerce, Washington, DC, 3rd edn., 1986.
- [12] *Bulletin 542*, US Bureau of Mines, 1954, cited in *Handbook of Chemistry and Physics*, CRC Press, Boca Raton, FL, 65th edn., 1988–1989, p. D 36.
- [13] D. Mehandjiev, *CR Acad. Bulgare Sci.*, **22** (1969) 1253.
- [14] B.J. Shau, P.C.S. Wu and P. Chiotti, *J. Nucl. Mater.*, **67** (1977) 13.
- [15] B. Malinowska, M. Cassir and J. Devynck, *J. Electrochem. Soc.*, **141** (1994) 2015.
- [16] B. Malinowska, M. Cassir and J. Devynck, *Solid State Ionics*, (1995) submitted for publication.
- [17] J. Morales, C. Pérez-Vicente and J.L. Tirado, *Mater. Res. Bull.*, **25** (1990) 623.
- [18] K. Hatoh, J. Niikura, E. Yasumoto and T. Gamo, *J. Electrochem. Soc.*, **141** (1994) 1725.
- [19] M. Armand, F. Dalard, D. Derou and C. Moulom, *Solid State Ionics*, **15** (1985) 205.
- [20] A.J. Bard and R. Faulkner, *Electrochemical Methods, Fundamentals and Applications*, Wiley, New York, 1980.
- [21] K. Ota, S. Mitsushima, S. Kato, S. Asano, H. Yoshitake and N. Kamiya, *J. Electrochem. Soc.*, **139** (1992) 667.